Research Paper

Machine learning-based B cell-related diagnostic biomarker signature and molecular subtypes characteristic of ulcerative colitis

Guo-Liang Wu[1,2], Li Li[3], Xiao-Yao Chen[2], Wei-Feng Zhang[4,5], Jun-Bo Wu[6], Xiaoning Yu[7], Hong-Jin Chen[5]

[1]First Clinical Medical College, Nanjing University of Chinese Medicine, Nanjing, Jiangsu 210023, China
[2]Department of Anorectal Section, The First Affiliated Hospital of Shandong First Medical University, Jinan, Shandong 250014, China
[3]Department of Endocrinology, The Affiliated Hospital of Shandong University of Traditional Chinese Medicine, Jinan, Shandong 250014, China
[4]Department of Colorectal Surgery, The Affiliated Hospital of Nanjing University of Chinese Medicine, Nanjing, Jiangsu 210029, China
[5]Department of Anorectal Section, The Affiliated Hospital of Xuzhou Medical University, Xuzhou, Jiangsu 221000, China
[6]Department of Colorectal Surgery, Hengyang Central Hospital, Hengyang, Hunan 421001, China
[7]Department of Geriatrics, Hematology and Oncology Unit, Qilu Hospital of Shandong University, Jinan, China

Correspondence to: Hong-Jin Chen, Xiaoning Yu; **email:** 260789@njucm.edu.cn; yuxiaoning7709@163.com, https://orcid.org/0009-0008-6441-2801
Keywords: ulcerative colitis, B cell-related genes, diagnostic biomarker, immune infiltration, machine learning
Received: October 10, 2023 **Accepted:** January 3, 2024 **Published:** February 5, 2024
Correction: This article has been corrected. Please see Aging 2024: https://doi.org/10.18632/aging.206209

ABSTRACT

As an inflammatory bowel disease, ulcerative colitis (UC) does not respond well to current treatments. It is of positive clinical significance to further study the pathogenesis of UC and find new therapeutic targets. B lymphocytes play an important role in the pathogenesis of UC. The effect of anti-CD20 therapy on UC also provides new evidence for the involvement of B cells in UC process additionally, suggesting the important role and potential therapeutic value of B cells in UC. In this study, we screened the most critical immune cell-related gene modules associated with UC and found that activated B cells were closely related to the gene modules. Subsequently, key activated B cell-associated gene (BRG) signatures were obtained based on WGCNA and differential expression analysis, and three overlapping BRG-associated genes were obtained by RF and LASSO algorithms as BRG-related diagnostic biomarkers for UC. Nomogram model was further performed to evaluate the diagnostic ability of BRG-related diagnostic biomarkers, subsequently followed by UC molecular subsets identification and immunoinfiltration analysis. We also further verified the expressions of the three screened BRGs *in vitro* by using an LPS-induced NCM460 cell line model. Our results provide new evidence and potential intervention targets for the role of B cells in UC from a new perspective.

INTRODUCTION

Ulcerative colitis (UC) is a chronic inflammatory bowel disease (IBD) that causes chronic diarrhea and rectal bleeding. The incidence of UC is increasing globally and has a significant impact on life expectancy [1]. The current first-line treatment for inducing and maintaining mild to moderate UC remission is 5-aminosalicylic acid. The latest treatment for moderate to severe ulcerative colitis is oral corticosteroid-induced remission, coupled with small molecule drugs such as anti-tumor necrosis factor, α4β7 integrin and Janus kinase inhibitors to maintain remission [2]. However, in clinical trials, the highest response range of UC patients to these drug treatments was only 30% to 60%. Many patients still require hospitalization and 10–20% require colectomy [3]. Therefore, it is of positive clinical significance to further study the pathogenesis of UC in order to obtain new therapeutic targets.

B lymphocytes play a crucial role in the pathogenesis of UC. B cells are responsible for antibody synthesis, antigen delivery to T cells, and regulation of inflammatory responses by secreting cytokines such as IL-2, IL-10, IFN-γ, and TGF-β [4]. The percentage of $CD23^+$ B cells increased in all UC patients [5]. There is evidence for the role of B cells in chronic inflammation, as well as abnormal B cell responses in UC patients [6]. B cells can be divided into effector cells that secrete antibodies and cytokines, and IL-10-secreting regulatory cells (Bregs) [7]. The reduction of Bregs was identified as a characteristic indicator of UC. The frequency of Bregs in peripheral blood and intestinal tissue was significantly reduced in UC patients [8]. Meanwhile, serum IL-10 levels in UC patients were negatively correlated with Mayo Clinic scores, CRP and ESR [8]. However, a clinical trial comparing the efficacy of B cell depletion therapy with placebo reported negative results, which requires further investigation of the role of B cells in UC and obtaining new relevant therapeutic targets [6].

In addition, the effect of anti-CD20 therapy on UC provides new evidence for the involvement of B cells in the UC process. As a transmembrane protein expressed in B cells, the effect of CD20-related therapy on UC has received increasing attention. Intestinal mucosal immunity depends on the balance between pro-inflammatory and anti-inflammatory stimuli of the immune system, and it has been shown that antigen presentation by B cells may be beneficial for UC [9]. B cells may have a protective effect in UC by producing the anti-inflammatory cytokine IL-10 [10, 11]. Monocytes in UC patients who were not treated with anti-CD20 rituximab (RTX) produced higher levels of IL-10 [12]. Since the clinical application of RTX, there have been reports of endogastrointestinal toxicity of UC caused by RTX [13, 14]. After stopping RTX and giving IBD-specific therapy, UC symptoms improved in most patients [15]. Anti-CD20 monoclonal antibodies lead to new onset of IBD through changes in the degree of inflammation and damage to the gastrointestinal mucosal immune environment [16]. The reduction of B cells is thought to underlie the maintenance of intestinal mucosal immune homeostasis and may underlie this adverse reaction [17]. Serum concentrations of TNF-α and IL-6 increased after RTX treatment, as did monocytes expressing TNF-α in the colon, suggesting that B cells may regulate TNF-α production in colon inflammation [18]. All these evidences suggest the important role and potential therapeutic value of B cells in UC. It has positive clinical significance for further research.

In this study, we screened the most critical immune cell-related gene modules associated with UC, and found that activated B cells were strongly correlated with gene modules. Based on WGCNA, differential expression analysis as well as RF and LASSO algorithms, key activated B cell-related gene (BRG) signatures were obtained and three BRGs were screened as UC diagnostic biomarkers. The LPS-induced NCM460 cell line model was also applied *in intro* to further verify the abnormal expressions of the three screened BRGs. Our results provide new evidence and potential intervention targets for the role of B cells in UC from a new perspective.

MATERIALS AND METHODS

Data download and batch effect removal

We downloaded four GEO datasets containing healthy (HC) and ulcerative colitis (UC) samples from the GEO database for the subsequent analysis. Among the four GEO datasets, GSE48634 (GPL10558, Illumina HumanHT-12 V4.0 expression beadchip) and GSE92415 (GPL13158, (HT_HG-U133_Plus_PM) Affymetrix HT HG-U133+ PM Array Plate) (90 HC and 122 UC samples) were combined as the training cohort. GSE179285 (GPL6480, Agilent-014850 Whole Human Genome Microarray 4x44K G4112F (Probe Name version)) and GSE107499 (GPL15207, (PrimeView) Affymetrix Human Gene Expression Array) (31 HC and 175 UC samples) were combined as the validation cohort. To remove the batch effect of each GEO dataset, we utilized the "SVA" package to standardize processing the transcriptome data [19, 20].

Immune cell proportion estimation and WGCNA development

According to the 23 types immune cell signatures, we utilized the "GSVA" package to estimate the Single

Sample Gene Set Enrichment Analysis (ssGSEA) score of 23 types immune cells proportion (Supplementary Table 1). Based on the "WGCNA" script, a WGNCA related model was constructed to identify the pivotal immune cell associated gene module. In first, an all-sample clustering tree was established to remove the abnormal samples and calculate the optimal soft threshold (β) to build the WGCNA. Utilizing the Pearson correlated algorithm, the potential association of each gene module and immune cells was evaluated and the most related gene module was selected for the final analysis.

Differential expression gene (DEGs) identification and molecular function enrichment analysis

With the selection threshold set at |FC| > 1.4 and *p*.adjust < 0.05, the DEGs between HC and UC groups were identified. "clusterProfiler" package was utilized to explore the potential molecular function of GO and KEGG terms. Based on the reference of "c2.cp.kegg. v7.4.symbols", a Gene Set Enrichment Analysis (GSEA) was carried out to predict the KEGG terms of HC and UC groups.

Machine learning algorithm to select the feature diagnostic biomarker and nomogram establishment

Utilizing the "glmnet" package, a LASSO model was established to identify the feature variables. Then, random forest (RF) algorithm was performed to calculate the importance of each variable. The overlapping genes obtained by RF and LASSO were identified as the feature diagnostic biomarker for UC. Based on the expression profile of the diagnostic biomarker, a nomogram model was established via "glmnet" package. The nomogram score was calculated using the formula: nomogram score = CHI3L1 × 0.33 + MMP7 × 0.48 + PCK1 × −0.35. Package "pROC" was employed to evaluate the diagnostic effectiveness of biomarker for UC.

Cell line model construction and quantitative real-time PCR (qRT-PCR)

The NCM460 cell line was cultured in RPMI-1640 medium (SH30809; HyClone, USA) supplemented with 10% fetal bovine serum (FBS; Sijiqing, Hangzhou, China) at 37°C in a humidified atmosphere containing 5% CO_2. NCM460 cells were seeded and then treated with lipopolysaccharide (LPS) at a concentration of 1 μg/ml (Sigma, USA) for 24 hours to create an *in vitro* model of ulcerative colitis (UC) cells. After 24 hours, the LPS-induced NCM460 cells were collected for further experiments. Total cellular RNA was extracted using Trizol (Cat#9109; TaKaRa, Japan), and cDNA was synthesized using the PrimeScript RT Master Mix kit (Cat#RR047A; Takara, Japan). The mRNA levels were quantified using SYBR Green PCR Mix (Cat#RR420A; Takara, Japan). Data analysis was performed using the $2^{-\Delta\Delta CT}$ method, and each experiment included three separate control sets.

Generation of molecular subgroups pattern

According the expression profile of diagnostic biomarker, a molecular subgroup pattern of UC samples was generated using "ConsensusClusterPlus" package. Based on the optimal classification of K = 2–9, the UC samples were divided into different molecular subgroups.

Statistical analysis

Data analysis and processing in this study were performed in R language environment. Correlation analysis between the two groups was calculated using Pearson algorithm. Statistical differences between the two groups were calculated using Wilcox rank-sum test. $p < 0.05$ was considered statistically significant. $^{*}p < 0.05$. $^{**}p < 0.01$, $^{***}p < 0.001$.

Data availability statement

The datasets generated and/or analyzed during the current study are available in the repositories of GEO.

RESULTS

Generation of the pivotal activated B cell-related gene module for UC sample

Two independent cohorts (GSE48634 and GSE92415) were included to identify the most pivotal immune cell related gene module associated with UC. After filtering the transcriptome data, all samples were clustered to exclude outlier samples. With the scale free topology model (R^2) set at 0.85, the soft threshold (β = 5) was set to establish the WGCNA (Figure 1A). Under the height of clustering tree set at 0.25, we clustered each gene module and the correlation result illustrated a weak relationship of each gene module (Figure 1B, 1C). The gene modules were subsequently cut by dynamic tree and merged the gene modules for the final analysis (Figure 1D). After the correlation evaluation of each gene module and 23 immune cell subtypes, a strong correlation was observed in most gene modules and immune cell subtypes, especially the yellow gene module and activated B cell (Figure 1E). The scatter dot analysis revealed a strong correlation between the module membership and gene significance in yellow module (r = 0.96, $p < 1e{-}200$), and this gene module was identified as the pivotal activated B cell-related gene module for UC (Figure 1F).

Identification of differential expression activated B cell-related gene signature and molecular pathway analysis

According to the differential expression analysis of HC and UC group, the DEGs were further identified via "limma" script (Figure 2A). Based on the WGCNA and differential expression analysis, a total of 32 pivotal activated B cell-related gene (BRGs) signatures were identified (Figure 2B). GO enrichment analysis suggested that the pivotal BRGs were involved in the activation of immune response, leukocyte mediated

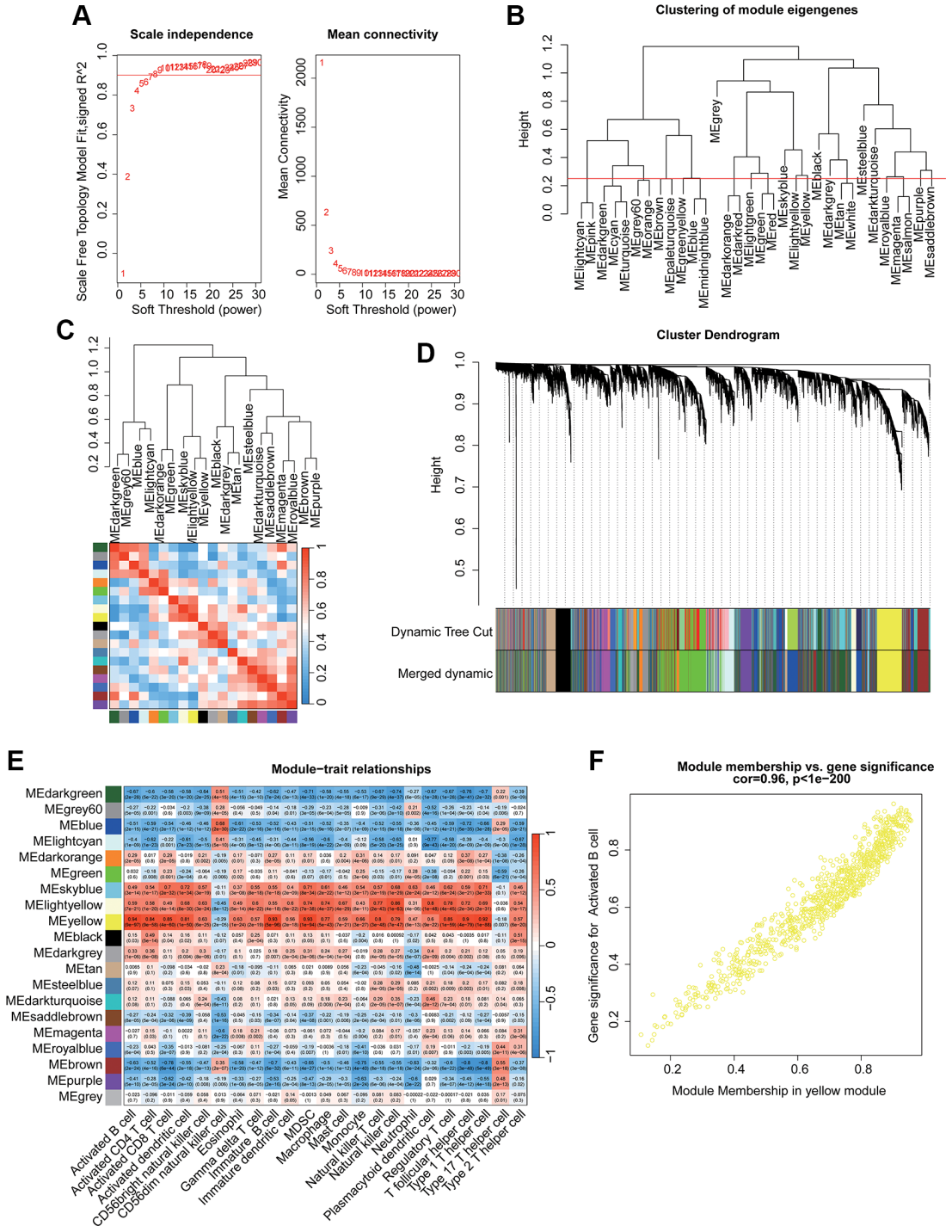

Figure 1. Identification the immune cell subtype related gene module for UC via WGCNA. (**A**) Identification of the optimal soft threshold (β) to develop the WGCNA. (**B**) Clustering of each gene module. (**C**) Correlation evaluation of each gene module. (**D**) Generation of the unique gene module via dynamic tree cut. (**E**) Correlation analysis of each gene module and 23 immune cell subtypes. (**F**) Relationship of module membership in yellow module and gene significance.

immunity, humoral immune response, external side of plasma membrane and carbohydrate binding (Figure 2C). The KEGG pathway result illustrated that the pivotal BRGs were related to chemokine signaling pathway, cytokine−cytokine receptor interaction, viral protein interaction with cytokine and cytokine receptor and B cell receptor signaling pathway (Figure 2D).

Investigation of BRGs related diagnostic biomarker via machine learning algorithm

LASSO and RF algorithms were utilized to identify the BRGs related diagnostic biomarker for UC. On the basis of LASSO analysis, 7 BRGs related gene signatures were selected according to the minimum log lambda and optimal coefficient (Figure 3A, 3B). Utilizing the RF algorithm, the importance of 32 pivotal BRGs related gene signatures was calculated and 17 important variables were selected (Figure 3C, 3D). Finally, 3 overlapping BRGs related gene signatures were obtained via RF and LASSO algorithms and were considered as the BRGs related diagnostic biomarkers for UC (Figure 3E). The correlation analysis revealed that CHI3L1 was positively related to MMP7 and negatively related to PCK1; MMP7 was negatively correlated with PCK1 (Figure 3F).

Diagnostic effectiveness evaluation of BRGs related biomarker and nomogram establishment

Two independent cohort (GSE179285 and GSE107499) were utilized to validate the expression and diagnostic ability of the BRGs related biomarkers for UC. In the training subgroup, the expressions of CHI3L1 and MMP7 were observed to be overexpressed in the UC group, whereas the expression of PCK1 was down-regulated in the UC group. Notably, the expression level of the BRGs related biomarkers in the validation subgroup was consisted with the training subgroup (Figure 4A–4F). Based on the expression profile of 3 BRGs related biomarkers, we subsequently developed a nomogram model to evaluate the diagnostic ability of BRGs related biomarkers in both training and validation subgroups. As shown in Figure 4G–4J, the AUCs of CHI3L1, PCK1, MMP7 and nomogram were 0.717, 0.725, 0.716 and 0.762 in the training subgroup and 0.741, 0.723, 0.663 and 0.722 in the validation subgroup.

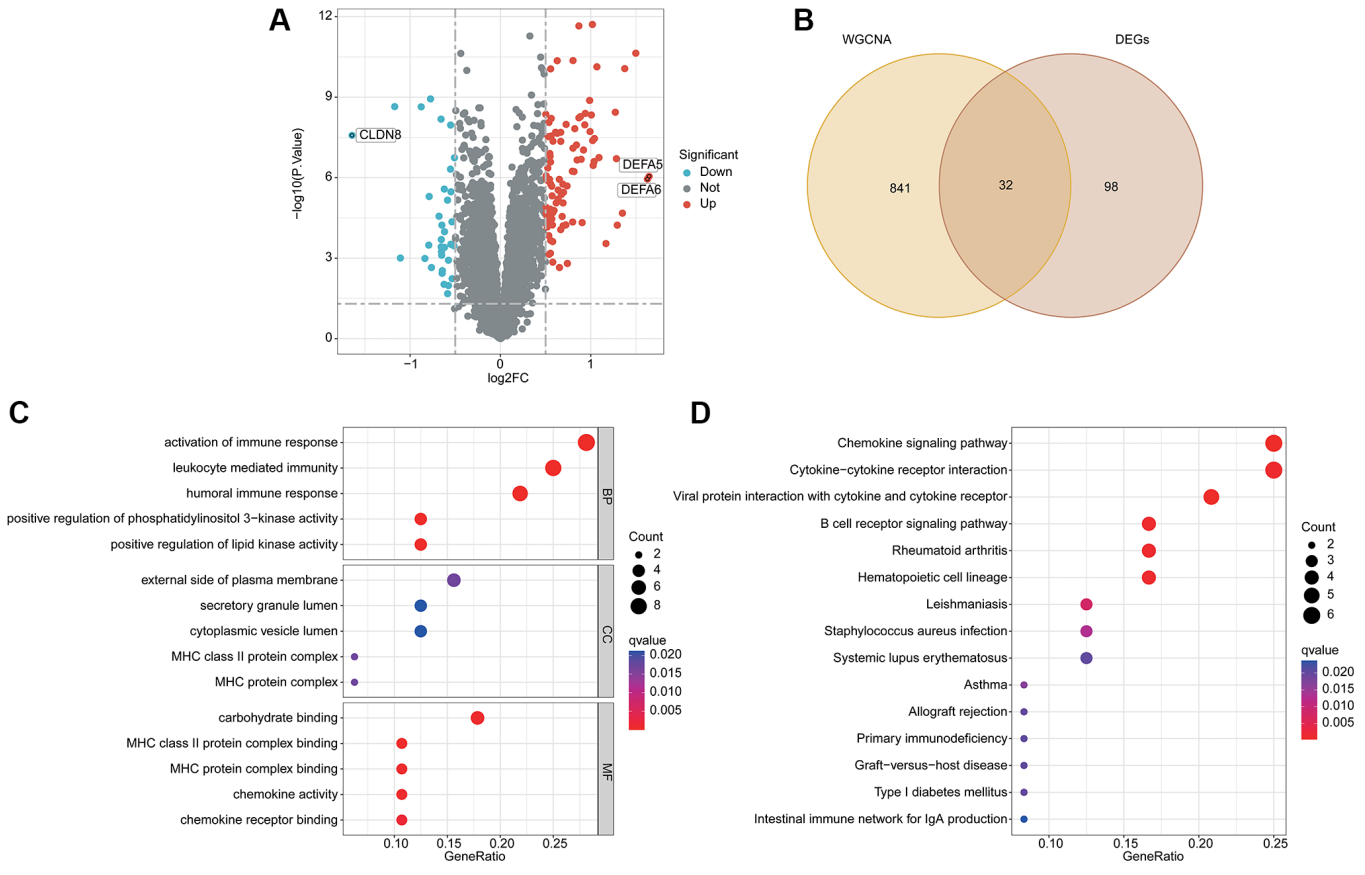

Figure 2. Analysis of differential expression BRGs and potential molecular pathway exploration. (**A**) Differential expression analysis by volcano plot. (**B**) Overlapping gene screening after WGCNA and differential expression analysis. (**C**) GO enrichment analysis. (**D**) The KEGG pathway analysis.

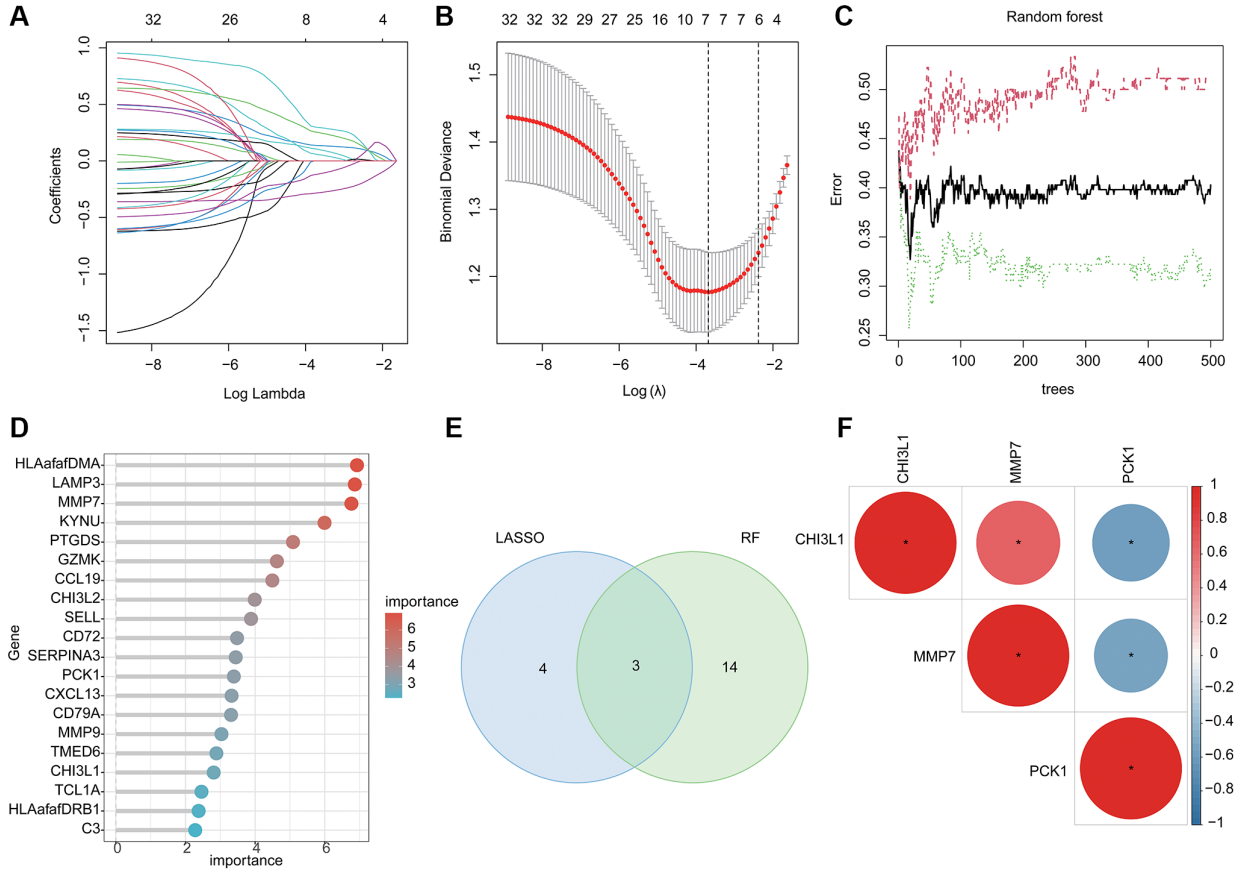

Figure 3. Machine learning based BRGs diagnostic biomarkers identification. (**A**, **B**) LASSO analysis of 32 pivotal BRGs related gene signatures. (**C**, **D**) The importance calculation of BRGs related gene signatures via RF algorithm. (**E**) Identification of BRGs related diagnostic biomarkers via RF and LASSO. (**F**) Potential correlation analysis of 3 BRGs related diagnostic biomarkers.

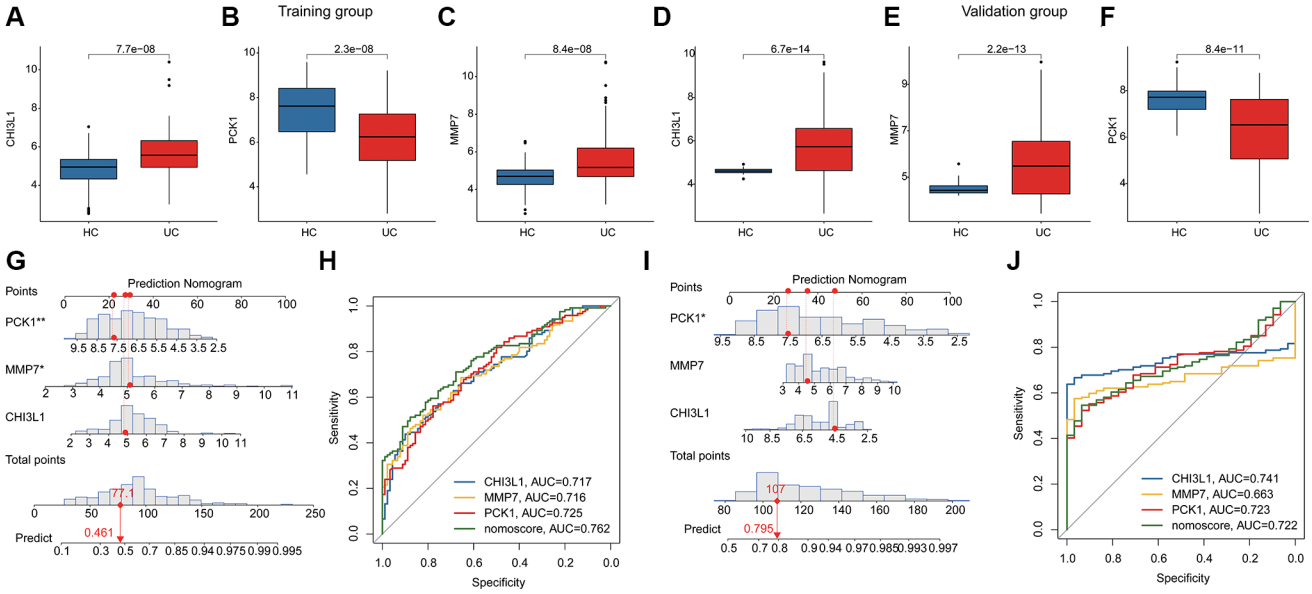

Figure 4. Diagnostic ability estimation and nomogram model development of BRGs related biomarkers in UC. (**A**–**F**) The expression level of BRGs related biomarkers of HC and UC samples in the training and validation subgroups. (**G**) Nomogram development of CHI3L1, PCK1, MMP7 in the training subgroup. (**H**) ROC analysis of BRGs related biomarkers and nomogram in the training subgroup. (**I**) Nomogram development of CHI3L1, PCK1, MMP7 in the validation subgroup. (**J**) ROC analysis of BRGs related biomarkers and nomogram in the validation subgroup.

Potential association of BRGs related biomarkers and immune infiltration characterization

We further conducted a GSEA analysis to reveal the potential molecular pathways. In HC group, the metabolic pathways related to some small molecules were significantly upregulated, involving butanoate metabolism, drug metabolism cytochrome p450 and fatty acid metabolism (Figure 5A). Additionally, a series of immune related molecular pathways was observed significantly upregulated in the UC group, such as chemokine signaling pathway, cytokine-cytokine receptor interaction and hematopoietic cell lineage (Figure 5B). The quantitative data of immune infiltration characterization suggested that most of the immune cells had higher expression levels in the UC group, such as activity B cell, $CD4^+$ T cell, $CD8^+$ T cell, activated dendritic cell, CD56 bright natural killer cell, immature B cell, MDSC, macrophage, monocyte, and natural killer T cell (Figure 5C). Principal component analysis (PCA) of the immune infiltration characterization revealed a clear distinction between HC and UC groups (Figure 5D). Correlation analysis of BRGs related biomarkers and immune infiltration characterization illustrated that the PCK1 was negatively associated with most immune

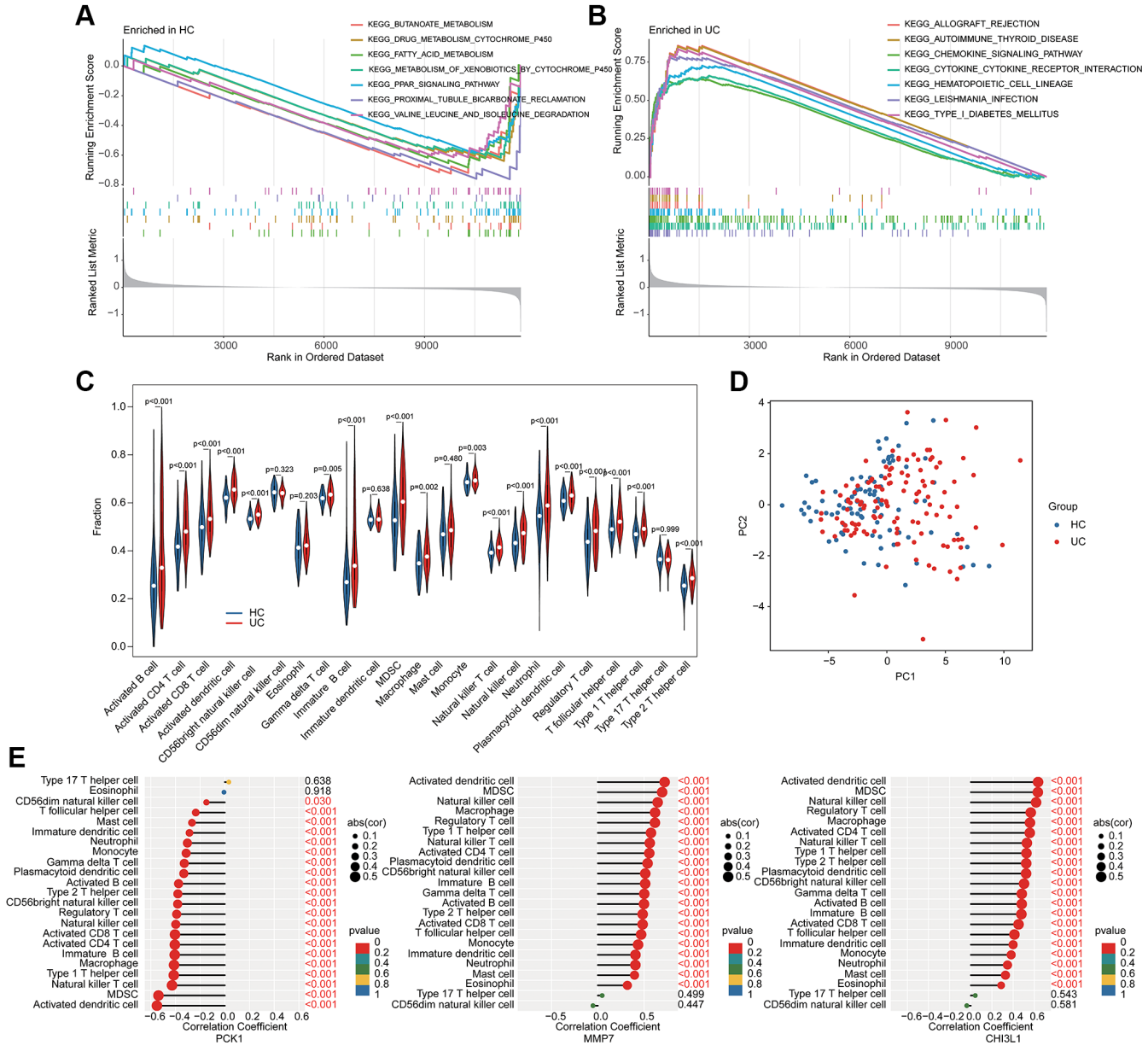

Figure 5. GSEA analysis and association analysis of immune infiltration characterization and BRGs related biomarkers. GSEA estimation of (**A**) HC group and (**B**) UC group. (**C**) Immune infiltration characterization evaluation. (**D**) PCA analysis of immune cells between HC and UC groups. (**E**) Potential association of 3 BRGs related biomarkers and immune infiltration characterization.

cells, whereas MMP7 and CHI3L1 were positively associated with most immune cells (Figure 5E). Collectively, these results demonstrated a significant difference in immune infiltration characterization between the HC and UC groups and the screened BRGs related biomarkers were closely associated with the immune infiltration.

Identification of molecular subgroup and immune infiltration analysis for UC

Based on the BRGs related biomarkers, we conducted a consensus clustering analysis of UC samples. Under the optimal classification of K = 2, the UC samples were classified into 2 molecular subgroups (Figure 6A–6C).

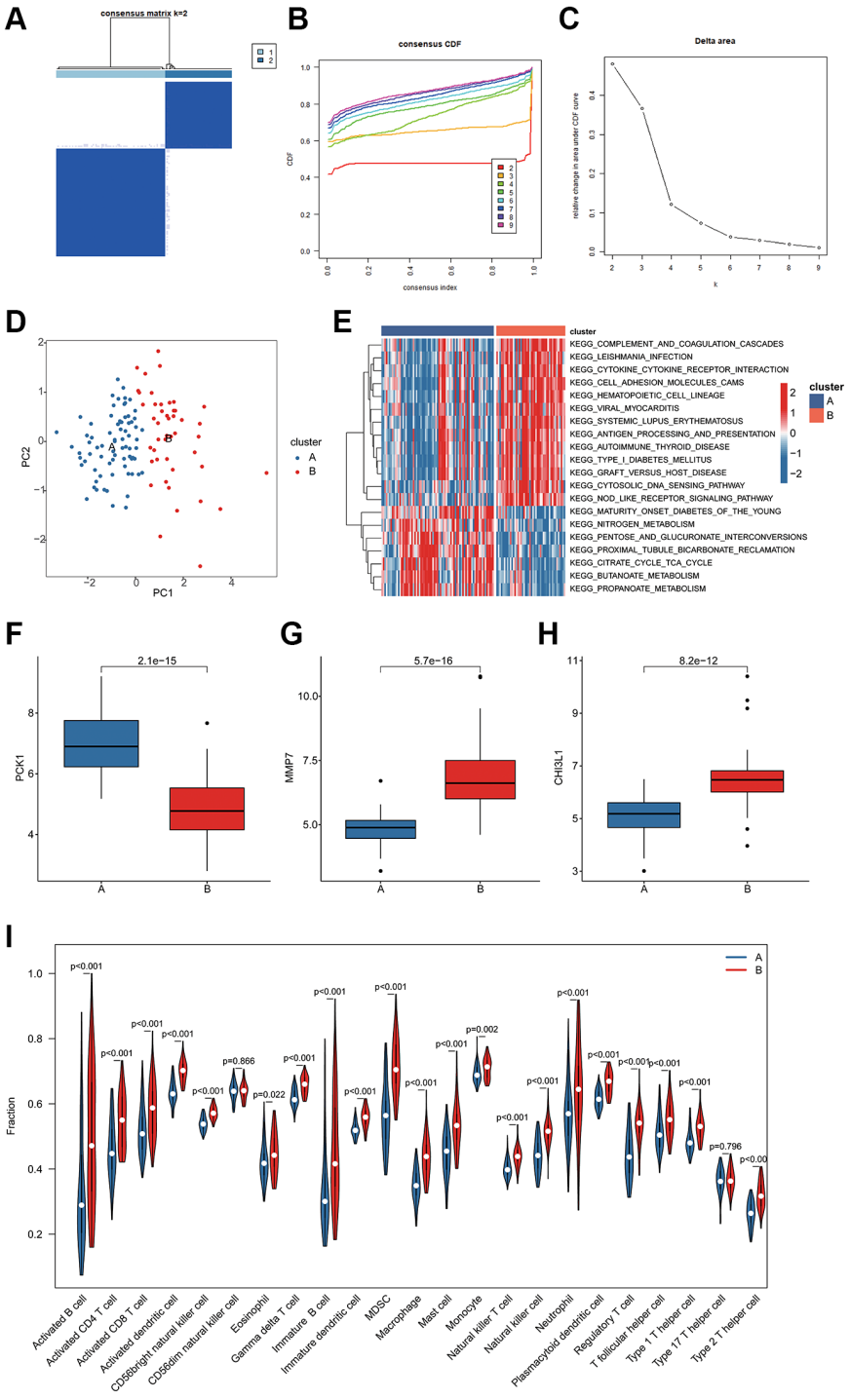

Figure 6. BRGs-based molecular subgroups identification and immune infiltration evaluation. (**A**–**C**) BRGs-based molecular subgroups generation. (**D**) PCA analysis of cluster A and B. (**E**) GSVA analysis of molecular pathways. (**F**–**H**) Expression profile of 3 BRGs related biomarkers of BRGs-based cluster subgroups. (**I**) Immune infiltration characterization of BRGs-based cluster subgroups.

The PCA diagram displayed a distinct distribution pattern of BRG-based cluster A and cluster B based on the BRGs related biomarkers (Figure 6D). The GSVA result suggested that a series of immune related molecular pathways were greatly upregulated in the cluster B, while some metabolism related molecular pathways were upregulated in the cluster A (Figure 6E). The BRGs related biomarkers expression profile revealed that the expression of PCK1 was down-expressed of UC samples in the cluster B, whereas the expressions of MMP7 and CHI3L1 were over-expressed of UC samples in cluster B (Figure 6F–6H). Immune infiltration analysis of BRGs-based molecular sub-groups illustrated that the UC samples in the cluster B had higher immune infiltration level, including activity B cell, $CD4^+$ T cell and $CD8^+$ T cell (Figure 6I).

In vitro qRT-PCR validation of BRGs related biomarkers

We further validated the expressions of 3 screened BRGs *in vitro* by LPS-induced NCM460 cell line model. As shown in Figure 7, the mRNA expression of CHI3L1 and MMP7 were significantly overexpressed, while PCK1 was obviously lower in the UC group.

DISCUSSION

As a clinical disease with poor therapeutic effect, the further study of UC has positive clinical significance. In this study, we screened B cell-associated UC diagnostic markers. In addition, immunosignature analysis and pathway enrichment analysis of UC patients provide possible clues for the involvement of UC prognosis.

In this study, we screened out three diagnostic markers of UC. Similar to the results of another multicenter study of intestinal gene expression differences, we also identified MMP7 as a differential upregulator of UC [21]. As a member of matrix metalloproteinase (MMP), MMP7 has proteolytic activity against a variety of substrates [22]. Defects in specific components of the mucosal barrier are one of the specific structural changes in UC patients and allow chronic mucosal inflammation to persist [23]. In UC, it has been reported that MMP-7 degraded the tight junction protein Claudin-7 in epithelial cells, which damaged the intestinal epithelial barrier and increases inflammation. Treatment with MMP-7 monoclonal antibody improved intestinal barrier function and reduced inflammation in rats [24]. This suggests MMP-7 as a potential therapeutic target for IBD.

Chitinase 3-like 1 (CHI3L1) belongs to the glycohydrolase 18 family of chitinases. CHI3L1 has been reported to enhance the ability of bacteria to adhere to and invade colon epithelial cells to exacerbate intestinal inflammation [25, 26]. Therefore, its expression is elevated in IBD patients and is accompanied by increasing disease activity [25, 27]. Some studies have even suggested that loss of tolerance to CHI3L1 is a characteristic of UC [28]. In addition, similar to MMP7, CHI3L1 expression is increased during the progression of colitis-associated carcinoma (CAC) [29]. Oxidative damage caused by CHI3L1 by inhibiting the increase in reactive oxygen species (ROS) induced by caffeine may be one of the reasons [30]. CHI3L1 was reported to be associated with infliximab/adalimumab and vedolizumab treatment response [31]. All these suggest the potential of CHI3L1 as an ideal target for clinical intervention.

We also identified phosphoenolpyruvate carboxykinase 1 (PCK1) as a differentially regulated gene for UC. PCK1, an enzyme involved in glucose production, also regulates adipogenesis and is associated with hepatic

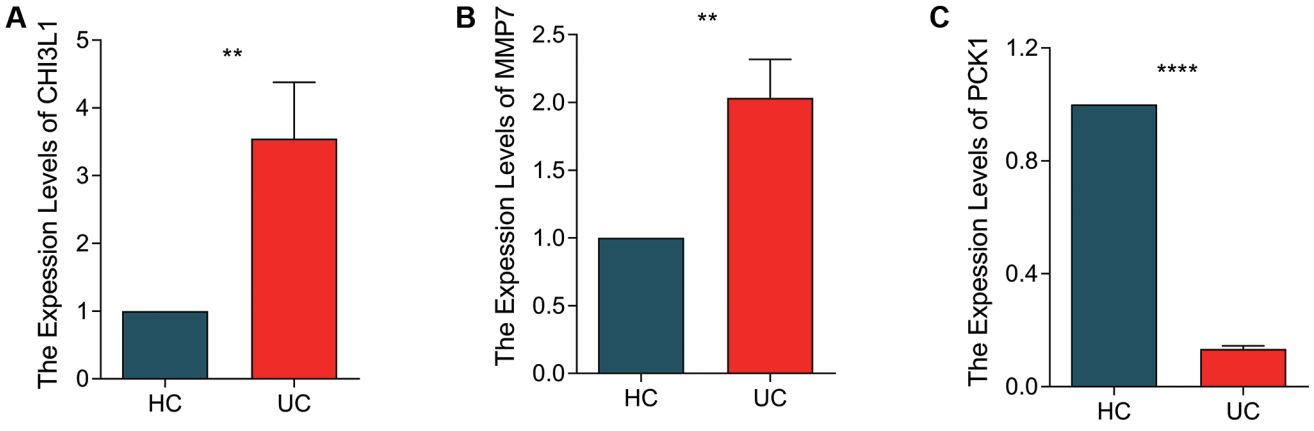

Figure 7. qRT-PCR validation of BRGs related biomarkers in NCM460 cell line and LPS-induced NCM460 cell line. The quantitative statistical analysis of expression levels of (**A**) CHI3L1, (**B**) MMP7 and (**C**) PCK1 in NCM460 and LPS-induced NVM460 cell lines. $^{*}p < 0.05$, $^{**}p < 0.01$, $^{***}p < 0.001$.

steatosis [32]. Although it has not been reported in depth in UC, there are clues to its role at UC. PCK1 contributes to M1 polarization in macrophages, suggesting the role of PCK1 in inhibiting inflammation [33]. In mouse models, the latest reports show that PCK1 knocked-out mice increased inflammatory infiltration and caused high levels of TNF-α. At the same time, PCK1 deficiency through the PI3K/AKT/PDGF axis significantly increased mRNA levels of genes associated with inflammation, which is in line with our result [34]. Given that the regulation of the PI3K/AKT axis has become a hot topic in IBD treatment research [35], PCK1 is expected to receive further attention.

Our results showed that molecular subtyping of BRGs showed that in addition to immune-related biological processes, including antigen processing and presentation, graft versus host disease, a variety of metabolism-related pathways were also enriched to be related to risk stratification, such as nitrogen metabolism, TCA, butanoate metabolism, propanoate metabolism. To satisfy cell growth and proliferation, the activation process of immune cells is accompanied by metabolic reprogramming [36]. In addition, metabolic reprogramming has also been shown to affect B cell differentiation [37]. Their interaction creates a complex link between BRGs and metabolism. Although there is some evidence suggesting the role of metabolic processes such as TCA in UC [38], the study of these metabolic processes in UC is still unveiled. Additionally, we have not been able to find evidence that B cells are involved in these metabolic pathways. But at the very least, our study sheds light on the role of metabolic pathways in UC risk stratification and the potential involvement of B cells in this process.

We observed a higher concentration of myeloid suppressor cells (MDSCs) in patients with UC. It was reported that increased frequency of MDSC was observed in peripheral blood of patients with IBD and could directly regulate IBD progression by regulating T cell function [39]. In addition, highly expressed MDSC is associated with worsening of IBD and an increased likelihood of cancer progression [40]. The mechanism may be that MDSC produces IL-10, which in turn promotes cancer initiation by regulating the STAT3-DNMT3b-IRF8 axis [41]. This may explain the increased incidence of colon cancer in UC patients. The intervention of MDSC to control UC disease progression has clinical application potential.

Another immune cell whose expression was significantly different in the immune microenvironment and significantly correlated with the expression level of the screened UC diagnostic markers in this study was dendritic cells (DCs). DC regulates responses to the gut microbiota by acting as a bridge between innate and adaptive immune responses, and is one of the core players in UC by influencing the mucosal immune system [42]. The level of DC expression is significantly decreased in patients with acute UC and correlated with disease activity [43]. TNF-a, IL-6, and IL-8 secreted by plasmacytoid dendritic cells (pDC) are also significantly increased in UC patients [44]. In addition, the $CD103^+$ DC subtype has an impaired ability to generate Treg cells while inducing a Th1/Th2/Th17 immune response that promotes UC development [45]. Therefore, a number of DC-associated proteins associated with UC genetic susceptibility have been identified as potential therapeutic targets [46]. At the same time, various immune-related treatments such as autophagy and probiotic regulation have also been shown to be associated with DC participation [47]. Our results showed that the three selected targets were significantly correlated with the expression level of DC, which also suggested the necessity of further exploring the function of DC in UC.

In summary, we found a strong correlation between activated B cells and UC immune cell-related gene modules, and obtained three BRGs as UC-related diagnostic biomarkers. Since the biomarker screening process in this study was based on public database, there was more of a correlation analysis than a causation analysis. Although *in vitro* experiments preliminarily verified the correlation between markers and UC to some extent, limited to conditions, the exact relationship between the screened markers and the established UC molecular subtypes cannot be established, and their molecular mechanisms were not further explored. Our results at least provide new evidence and potential intervention targets for the role of B cells in UC. In the future, further clinical validation and *in vitro* and *in vivo* experimental analysis will help to deepen this study.

AUTHOR CONTRIBUTIONS

HJC conceptualized and designed the study. GLW, LL and XYC performed data analysis, and validated the findings through *in vitro* experiments. WFZ and JBW contributed significantly to data collection and generated the tables and figures presented in this manuscript. All authors made substantial contributions to this article and have approved the submitted version.

CONFLICTS OF INTEREST

The authors declare no conflicts of interest related to this study.

FUNDING

This research was sponsored by Shandong Traditional Chinese Medicine Science and Technology Program (2020M048).

REFERENCES

1. Salvatori S, Neri B, Marafini I, Brigida M, Monteleone G. Emerging oral drug options for ulcerative colitis. Expert Opin Emerg Drugs. 2023; 28:191–201. https://doi.org/10.1080/14728214.2023.2254686 PMID:37668153

2. Gros B, Kaplan GG. Ulcerative Colitis in Adults: A Review. JAMA. 2023; 330:951–65. https://doi.org/10.1001/jama.2023.15389 PMID:37698559

3. Le Berre C, Honap S, Peyrin-Biroulet L. Ulcerative colitis. Lancet. 2023; 402:571–84. https://doi.org/10.1016/S0140-6736(23)00966-2 PMID:37573077

4. Sun X, Huang Y, Zhang YL, Qiao D, Dai YC. Research advances of vasoactive intestinal peptide in the pathogenesis of ulcerative colitis by regulating interleukin-10 expression in regulatory B cells. World J Gastroenterol. 2020; 26:7593–602. https://doi.org/10.3748/wjg.v26.i48.7593 PMID:33505138

5. Rabe H, Malmquist M, Barkman C, Östman S, Gjertsson I, Saalman R, Wold AE. Distinct patterns of naive, activated and memory T and B cells in blood of patients with ulcerative colitis or Crohn's disease. Clin Exp Immunol. 2019; 197:111–29. https://doi.org/10.1111/cei.13294 PMID:30883691

6. Ben-Horin S. Randomised placebo-controlled trial of rituximab (anti-CD20) in active ulcerative colitis. Gut. 2012; 61:327. https://doi.org/10.1136/gutjnl-2011-300398 PMID:21613645

7. Kałużna A, Olczyk P, Komosińska-Vassev K. The Role of Innate and Adaptive Immune Cells in the Pathogenesis and Development of the Inflammatory Response in Ulcerative Colitis. J Clin Med. 2022; 11:400. https://doi.org/10.3390/jcm11020400 PMID:35054093

8. Wang X, Zhu Y, Zhang M, Wang H, Jiang Y, Gao P. Ulcerative Colitis Is Characterized by a Decrease in Regulatory B Cells. J Crohns Colitis. 2016; 10:1212–23. https://doi.org/10.1093/ecco-jcc/jjw074 PMID:26980839

9. Mizoguchi E, Mizoguchi A, Preffer FI, Bhan AK. Regulatory role of mature B cells in a murine model of inflammatory bowel disease. Int Immunol. 2000; 12:597–605. https://doi.org/10.1093/intimm/12.5.597 PMID:10784605

10. Klug M, Apter S, Eshet Y, Marom EM. Ulcerative Colitis Exacerbation after Rituximab Treatment in Posttransplant Lymphoproliferative Disease. Radiol Imaging Cancer. 2022; 4:e220033. https://doi.org/10.1148/rycan.220033 PMID:35776002

11. Del Sordo R, Lougaris V, Bassotti G, Armuzzi A, Villanacci V. Therapeutic agents affecting the immune system and drug-induced inflammatory bowel disease (IBD): A review on etiological and pathogenetic aspects. Clin Immunol. 2022; 234:108916. https://doi.org/10.1016/j.clim.2021.108916 PMID:34971840

12. Goetz M, Atreya R, Ghalibafian M, Galle PR, Neurath MF. Exacerbation of ulcerative colitis after rituximab salvage therapy. Inflamm Bowel Dis. 2007; 13:1365–8. https://doi.org/10.1002/ibd.20215 PMID:17604367

13. Lee HH, Sritharan N, Bermingham D, Strey G. Ocrelizumab-Induced Severe Colitis. Case Rep Gastrointest Med. 2020; 2020:8858378. https://doi.org/10.1155/2020/8858378 PMID:33354373

14. Mallepally N, Abu-Sbeih H, Ahmed O, Chen E, Shafi MA, Neelapu SS, Wang Y. Clinical Features of Rituximab-associated Gastrointestinal Toxicities. Am J Clin Oncol. 2019; 42:539–45. https://doi.org/10.1097/COC.0000000000000553 PMID:31136371

15. Eckmann JD, Chedid V, Quinn KP, Bonthu N, Nehra V, Raffals LE. De Novo Colitis Associated With Rituximab in 21 Patients at a Tertiary Center. Clin Gastroenterol Hepatol. 2020; 18:252–3. https://doi.org/10.1016/j.cgh.2019.03.027 PMID:30905719

16. Tolaymat S, Sharma K, Kagzi Y, Sriwastava S. Anti-CD20 monoclonal antibody (mAb) therapy and colitis: A case series and review. Mult Scler Relat Disord. 2023; 75:104763. https://doi.org/10.1016/j.msard.2023.104763 PMID:37229799

17. Quesada-Simó A, Garrido-Marín A, Nos P, Gil-Perotín S. Impact of Anti-CD20 therapies on the immune homeostasis of gastrointestinal mucosa and their relationship with *de novo* intestinal bowel disease in multiple sclerosis: a review. Front Pharmacol. 2023; 14:1186016.

https://doi.org/10.3389/fphar.2023.1186016
PMID:37324473

18. Moritoki Y, Lian ZX, Lindor K, Tuscano J, Tsuneyama K, Zhang W, Ueno Y, Dunn R, Kehry M, Coppel RL, Mackay IR, Gershwin ME. B-cell depletion with anti-CD20 ameliorates autoimmune cholangitis but exacerbates colitis in transforming growth factor-beta receptor II dominant negative mice. Hepatology. 2009; 50:1893–903.
https://doi.org/10.1002/hep.23238
PMID:19877182

19. Leek JT, Johnson WE, Parker HS, Jaffe AE, Storey JD. The sva package for removing batch effects and other unwanted variation in high-throughput experiments. Bioinformatics. 2012; 28:882–3.
https://doi.org/10.1093/bioinformatics/bts034
PMID:22257669

20. Shu Q, She H, Chen X, Zhong L, Zhu J, Fang L. Identification and experimental validation of mitochondria-related genes biomarkers associated with immune infiltration for sepsis. Front Immunol. 2023; 14:1184126.
https://doi.org/10.3389/fimmu.2023.1184126
PMID:37228596

21. Noble CL, Abbas AR, Cornelius J, Lees CW, Ho GT, Toy K, Modrusan Z, Pal N, Zhong F, Chalasani S, Clark H, Arnott ID, Penman ID, et al. Regional variation in gene expression in the healthy colon is dysregulated in ulcerative colitis. Gut. 2008; 57:1398–405.
https://doi.org/10.1136/gut.2008.148395
PMID:18523026

22. Puthenedam M, Wu F, Shetye A, Michaels A, Rhee KJ, Kwon JH. Matrilysin-1 (MMP7) cleaves galectin-3 and inhibits wound healing in intestinal epithelial cells. Inflamm Bowel Dis. 2011; 17:260–7.
https://doi.org/10.1002/ibd.21443
PMID:20812334

23. Michielan A, D'Incà R. Intestinal Permeability in Inflammatory Bowel Disease: Pathogenesis, Clinical Evaluation, and Therapy of Leaky Gut. Mediators Inflamm. 2015; 2015:628157.
https://doi.org/10.1155/2015/628157
PMID:26582965

24. Xiao Y, Lian H, Zhong XS, Krishnachaitanya SS, Cong Y, Dashwood RH, Savidge TC, Powell DW, Liu X, Li Q. Matrix metalloproteinase 7 contributes to intestinal barrier dysfunction by degrading tight junction protein Claudin-7. Front Immunol. 2022; 13:1020902.
https://doi.org/10.3389/fimmu.2022.1020902
PMID:36275703

25. Mizoguchi E. Chitinase 3-like-1 exacerbates intestinal inflammation by enhancing bacterial adhesion and invasion in colonic epithelial cells. Gastroenterology. 2006; 130:398–411.
https://doi.org/10.1053/j.gastro.2005.12.007
PMID:16472595

26. Low D, Tran HT, Lee IA, Dreux N, Kamba A, Reinecker HC, Darfeuille-Michaud A, Barnich N, Mizoguchi E. Chitin-binding domains of Escherichia coli ChiA mediate interactions with intestinal epithelial cells in mice with colitis. Gastroenterology. 2013; 145:602–12.e9.
https://doi.org/10.1053/j.gastro.2013.05.017
PMID:23684751

27. Koutroubakis IE, Petinaki E, Dimoulios P, Vardas E, Roussomoustakaki M, Maniatis AN, Kouroumalis EA. Increased serum levels of YKL-40 in patients with inflammatory bowel disease. Int J Colorectal Dis. 2003; 18:254–9.
https://doi.org/10.1007/s00384-002-0446-z
PMID:12673492

28. Deutschmann C, Roggenbuck D, Schierack P. The loss of tolerance to CHI3L1 - A putative role in inflammatory bowel disease? Clin Immunol. 2019; 199:12–7.
https://doi.org/10.1016/j.clim.2018.12.005
PMID:30543919

29. Chen CC, Pekow J, Llado V, Kanneganti M, Lau CW, Mizoguchi A, Mino-Kenudson M, Bissonnette M, Mizoguchi E. Chitinase 3-like-1 expression in colonic epithelial cells as a potentially novel marker for colitis-associated neoplasia. Am J Pathol. 2011; 179:1494–503.
https://doi.org/10.1016/j.ajpath.2011.05.038
PMID:21763261

30. Ma JY, Li RH, Huang K, Tan G, Li C, Zhi FC. Increased expression and possible role of chitinase 3-like-1 in a colitis-associated carcinoma model. World J Gastroenterol. 2014; 20:15736–44.
https://doi.org/10.3748/wjg.v20.i42.15736
PMID:25400457

31. Shi Y, He W, Zhong M, Yu M. MIN score predicts primary response to infliximab/adalimumab and vedolizumab therapy in patients with inflammatory bowel diseases. Genomics. 2021; 113:1988–98.
https://doi.org/10.1016/j.ygeno.2021.04.011
PMID:33872704

32. Jiang H, Zhu L, Xu D, Lu Z. A newly discovered role of metabolic enzyme PCK1 as a protein kinase to promote cancer lipogenesis. Cancer Commun (Lond). 2020; 40:389–94.
https://doi.org/10.1002/cac2.12084
PMID:32809272

33. Ko CW, Counihan D, Wu J, Hatzoglou M, Puchowicz MA, Croniger CM. Macrophages with a deletion of

the *phosphoenolpyruvate carboxykinase 1* (*Pck1*) gene have a more proinflammatory phenotype. J Biol Chem. 2018; 293:3399–409.
https://doi.org/10.1074/jbc.M117.819136
PMID:29317502

34. Ye Q, Liu Y, Zhang G, Deng H, Wang X, Tuo L, Chen C, Pan X, Wu K, Fan J, Pan Q, Wang K, Huang A, Tang N. Deficiency of gluconeogenic enzyme PCK1 promotes metabolic-associated fatty liver disease through PI3K/AKT/PDGF axis activation in male mice. Nat Commun. 2023; 14:1402.
https://doi.org/10.1038/s41467-023-37142-3
PMID:36918564

35. Jalil AT, Hassan NF, Abdulameer SJ, Farhan ZM, Suleiman AA, Al-Azzawi AK, Zabibah R, Fadhil A. Phosphatidylinositol 3-kinase signaling pathway and inflammatory bowel disease: Current status and future prospects. Fundam Clin Pharmacol. 2023; 37:910–7.
https://doi.org/10.1111/fcp.12894
PMID:36939850

36. Pearce EL, Poffenberger MC, Chang CH, Jones RG. Fueling immunity: insights into metabolism and lymphocyte function. Science. 2013; 342:1242454.
https://doi.org/10.1126/science.1242454
PMID:24115444

37. Haniuda K, Fukao S, Kitamura D. Metabolic Reprogramming Induces Germinal Center B Cell Differentiation through Bcl6 Locus Remodeling. Cell Rep. 2020; 33:108333.
https://doi.org/10.1016/j.celrep.2020.108333
PMID:33147467

38. Ooi M, Nishiumi S, Yoshie T, Shiomi Y, Kohashi M, Fukunaga K, Nakamura S, Matsumoto T, Hatano N, Shinohara M, Irino Y, Takenawa T, Azuma T, Yoshida M. GC/MS-based profiling of amino acids and TCA cycle-related molecules in ulcerative colitis. Inflamm Res. 2011; 60:831–40.
https://doi.org/10.1007/s00011-011-0340-7
PMID:21523508

39. Haile LA, von Wasielewski R, Gamrekelashvili J, Krüger C, Bachmann O, Westendorf AM, Buer J, Liblau R, Manns MP, Korangy F, Greten TF. Myeloid-derived suppressor cells in inflammatory bowel disease: a new immunoregulatory pathway. Gastroenterology. 2008; 135:871–81.
https://doi.org/10.1053/j.gastro.2008.06.032
PMID:18674538

40. Flohr H, Breull W. Effect of etafenone on total and regional myocardial blood flow. Arzneimittelforschung. 1975; 25:1400–3.
PMID:23

41. Camici G, Manao G, Ramponi G. Nonenzymatic reactivation of des-acetyl citrate lyase by acetyl adenylate. First example of enzyme activation by chemotrophic modification. Physiol Chem Phys. 1975; 7:409–14.
PMID:698

42. Bernardo D, Chaparro M, Gisbert JP. Human Intestinal Dendritic Cells in Inflammatory Bowel Diseases. Mol Nutr Food Res. 2018; 62:e1700931.
https://doi.org/10.1002/mnfr.201700931
PMID:29336524

43. Baumgart DC, Metzke D, Schmitz J, Scheffold A, Sturm A, Wiedenmann B, Dignass AU. Patients with active inflammatory bowel disease lack immature peripheral blood plasmacytoid and myeloid dendritic cells. Gut. 2005; 54:228–36.
https://doi.org/10.1136/gut.2004.040360
PMID:15647187

44. Baumgart DC, Metzke D, Guckelberger O, Pascher A, Grötzinger C, Przesdzing I, Dörffel Y, Schmitz J, Thomas S. Aberrant plasmacytoid dendritic cell distribution and function in patients with Crohn's disease and ulcerative colitis. Clin Exp Immunol. 2011; 166:46–54.
https://doi.org/10.1111/j.1365-2249.2011.04439.x
PMID:21762123

45. Matsuno H, Kayama H, Nishimura J, Sekido Y, Osawa H, Barman S, Ogino T, Takahashi H, Haraguchi N, Hata T, Matsuda C, Yamamoto H, Uchino M, et al. CD103+ Dendritic Cell Function Is Altered in the Colons of Patients with Ulcerative Colitis. Inflamm Bowel Dis. 2017; 23:1524–34.
https://doi.org/10.1097/MIB.0000000000001204
PMID:28700533

46. Maneksha S, Harry TV. Lorazepam in sexual disorders. Br J Clin Pract. 1975; 29:175–6.
PMID:29

47. Sun D, Li C, Chen S, Zhang X. Emerging Role of Dendritic Cell Intervention in the Treatment of Inflammatory Bowel Disease. Biomed Res Int. 2022; 2022:7025634.
https://doi.org/10.1155/2022/7025634
PMID:36262975

SUPPLEMENTARY MATERIALS

Supplementary Table

Supplementary Table 1. The gene marker of the 23 types of immune cell.

Activated B cell:	ADAM28 CD180 CD79B BLK CD19 MS4A1 TNFRSF17 IGHM GNG7 MICAL3 SPIB HLA-DOB IGKC PNOC FCRL2 BACH2 CR2 TCL1A AKNA ARHGAP25 CCL21 CD27 CD38 CLEC17A CLEC9A CLECL1
Activated CD4 T cell:	AIM2 BIRC3 BRIP1 CCL20 CCL4 CCL5 CCNB1 CCR7 DUSP2 ESCO2 ETS1 EXO1 EXOC6 IARS ITK KIF11 KNTC1 NUF2 PRC1 PSAT1 RGS1 RTKN2 SAMSN1 SELL TRAT1
Activated CD8 T cell:	ADRM1 AHSA1 C1GALT1C1 CCT6B CD37 CD3D CD3E CD3G CD69 CD8A CETN3 CSE1L GEMIN6 GNLY GPT2 GZMA GZMH GZMK IL2RB LCK MPZL1 NKG7 PIK3IP1 PTRH2 TIMM13 ZAP70
Activated dendritic cell:	ABCD1 C1QC CAPG CCL3L3 CD207 CD302 ATP5B ATP5L ATP6V1A BCL2L1 C1QB SNURF SPCS3 CCNA1 CEACAM8 NOS2 SRA1 TNFRSF6B TREM1 TREML1 RHOA SLC25A37 TNFSF14 TREML4 VNN2 XPO6 CLEC4C TNFAIP2 UBD ACTR3 RAB1A SLA HLA-DQA2 SIGLEC5 SLAMF9
CD56bright natural killer cell:	ABAT C11orf75 C5orf15 CDHR1 DCAF12 DYNLL1 GPR137B HCP5 HDGFRP2 KRT86 MLST8 ELMOD3 ENTPD5 FAM119A FAM179A CLIC2 COX7A2L CREB3L4 CSF1 CSNK2A2 CSTA CSTB CTPS CTSD FST GATA2 GMPR HDC HEY1 HOXA1 HS2ST1 HS3ST1 BCL11B CDH3 MYL6B NAA16 ClQA ClQB CYP27B1 EIF3M
CD56dim natural killer cell:	CYP27A1 DDX55 DYRK2 RPL37A NOTCH3 AKR7A3 GPRC5C GRIN1 HLA-E PORCN PSMC4 UPP1 IL21R KIR2DS1 KIR2DS2 KIR2DS5
Eosinophil:	GIPR KRT18P50 LRMP FOSB RRP12 GPR183 NR4A3 ST3GAL6 DEPDC5 PDE6C PKD2L2 GPR65 IL5RA P2RY14 DACH1 DAPK2 EMR3
Gamma delta T cell:	ACP5 AQP9 BTN3A2 C1orf54 CARD8 CCL18 CD209 CD33 CD36 CDK5 IL10RB KLRF1 LGALS1 MAPK7 KLHL7 KRT80 LAMC1 LCORL LMNB1 MEIS3P1 MPL FABP1 FABP5 FADD MFAP3L MINPP1 RPS24 RPS7 RPS9 DBNL CCL13
Immature B cell:	CD22 CYBB FAM129C FCRL1 FCRL3 FCRL5 FCRLA HDAC9 HLA-DQA1 HVCN1 KIAA0226 NCF1 NCF1B P2RY10 SP100 TXNIP STAP1 TAGAP ZCCHC2
Immature dendritic cell:	ACADM AHCYL1 ALDH1A2 ALDH3A2 ALDH9A1 ALOX15 AMT ARL1 ATIC ATP5A1 CAPZA1 LILRA5 RDX RRAGD TACSTD2 INPP5F RAB38 PLAU CSF3R SLC18A2 AMPD2 CLTB C1orf162
MDSC:	CCR2 CD14 CD2 CD86 CXCR4 FCGR2A FCGR2B FCGR3A FERMT3 GPSM3 IL18BP IL4R ITGAL ITGAM PARVG PSAP PTGER2 PTGES2 S100A8 S100A9
Macrophage:	AIF1 CCL1 CCL14 CCL23 CCL26 CD300LB CNR1 CNR2 EIF1 EIF4A1 FPR1 FPR2 FRAT2 GPR27 GPR77 RNASE2 MS4A2 BASP1 IGSF6 HK3 VNN1 FES NPL FZD2 FAM198B HNMT SLC15A3 CD4 TXNDC3 FRMD4A CRYBB1 HRH1 WNT5B

Mast cell: ADAMTS3 CPA3 CMA1 CTSG ARHGAP15 CPM FCN1 FTL HSPA6 ITGA9 RNASE3 S100A4 SIGLEC8 SLC6A4 PTGS2 EGR3 PILRA

Monocyte: ASGR2 CFP ASGR1 CD1D UPK3A ACTG1 ANXA5 ATP6V1B2 CFL1 DAZAP2 CTBS EMR4P HIVEP2 MARCKSL1 MBP MMP15 PNPLA6 TMBIM6 PQBP1 TEX264 IKZF1

Natural killer T cell: BTN2A2 CD101 CD109 CNPY3 CNPY4 CREB1 CRTC2 CRTC3 CSF2 KLRC1 FUT4 ICAM2 IL32 LAMP2 LILRB5 KLRG1 HSPA4 HSPB6 ISM2 ITIH2 KDM4C KIR2DS4 KIRREL3 SDCBP NFATC2IP MICB KIR2DL1 KIR2DL3 KIR3DL1 KIR3DL2 NCR1 FOSL1 TSLP SLC7A7 SPP1 TREM2 UBASH3A YBX2 CCDC88A CLEC1A THBD PDPN VCAM1 EMR1

Natural killer cell: AKT3 AXL BST2 CDH2 CRTAM CSF2RA CTSZ CXCL1 CYTH1 DAXX DGKH DLL4 DPYD ERBB3 F11R FAM27A FAM49A FASLG FCGR1A FN1 FSTL1 FUCA1 GBP3 GLS2 GRB2 LST1 BCL2 CDC5L FGF18 FUT5 FZR1 GAGE2 IGFBP5 KANK2 LDB3

Neutrophil: CREB5 CDA CHST15 S100A12 APOBEC3A CASP5 MMP25 HAL C1orf183 FFAR2 MAK CXCR1 STEAP4 MGAM BTNL8 CXCR2 TNFRSF10C VNN3

Plasmacytoid dendritic cell: CBX6 DAB2 DDX17 HIGD1A IDH3A IL3RA MAGED1 NUCB2 OFD1 OGT PDIA4 SERTAD2 SIRPA TMED2 ENG FCAR IGF1 ITGA2B GABARAP GPX1 KRT23 PROK2 RALB RETNLB RNF141 SEC14L1 SEPX1 EMP3 CD300LF ABTB1 KLHL21 PHRF1

Regulatory T cell: CCL3L1 CD72 CLEC5A FOXP3 ITGA4 L1CAM LIPA LRP1 LRRC42 MARCO MMP12 MNDA MRC1 MS4A6A PELO PLEK PRSS23 PTGIR ST8SIA4 STAB1

T follicular helper cell: B3GAT1 CDK5R1 PDCD1 BCL6 CD200 CD83 CD84 FGF2 GPR18 CEBPA CECR1 CLEC10A CLEC4A CSF1R CTSS DMN DPP4 LRRC32 MC5R MICA NCAM1 NCR2 NRP1 PDCD1LG2 PDCD6 PRDX1 RAE1 RAET1E SIGLEC7 SIGLEC9 TYRO3 CHST12 CLIC3 IVNS1ABP KIR2DL2 LGMN

Type 1 T helper cell: CD70 TBX21 ADAM8 AHCYL2 ALCAM B3GALNT1 BBS12 BST1 CD151 CD47 CD48 CD52 CD53 CD59 CD6 CD68 CD7 CD96 CFHR3 CHRM3 CLEC7A COL23A1 COL4A4 COL5A3 DAB1 DLEU7 DOC2B EMP1 F12 FURIN GAB3 GATM GFPT2 GPR25 GREM2 HAVCR1 HSD11B1 HUNK IGF2 RCSD1 RYR1 SAV1 SELE SELP SH3KBP1 SIT1 SLC35B3 SIGLEC10 SKAP1 THUMPD2 TIGIT ZEB2 ENC1 FAM134B FBXO30 FCGR2C STAC LTC4S MAN1B1 MDH1 MMD RGS16 IL12A P2RX5 CD97 ITGB4 ICAM3 METRNL TNFRSF1A IRF1 HTR2B CALD1 MOCOS TRAF3IP2 TLR8 TRAF1 DUSP14

Type 17 T helper cell: IL17A IL17RA C2CD4A C2CD4B CA2 CCDC65 CEACAM3 IL17C IL17F IL17RC IL17RE IL23A ILDR1 LONRF3 SH2D6 TNIP2 ABCA1 ABCB1 ADAMTS12 ANK1 ANKRD22 B3GALT2 CAMTA1 CCR9 CD40 GPR44 IFT80

Type 2 T helper cell: ASB2 CSRP2 DAPK1 DLC1 DNAJC12 DUSP6 GNAI1 LAMP3 NRP2 OSBPL1A PDE4B PHLDA1 PLA2G4A RAB27B RBMS3 RNF125 TMPRSS3 GATA3 BIRC5 CDC25C CDC7 CENPF CXCR6 DHFR EVI5 GSTA4 HELLS IL26 LAIR2